Thermal stability and atomic ordering of epitaxial Heusler alloy Co_2FeSi films grown on GaAs(001)

M. Hashimoto, J. Herfort, H.-P. Schönherr, and K. H. Ploog
Paul-Drude-Institut für Festkörperelektronik, Hausvogteiplatz 5-7, D-10117 Berlin, Germany

(Received 11 July 2005; accepted 17 October 2005; published online 28 November 2005)

The thermal stability and the atomic ordering of single-crystal Heusler alloy Co_2FeSi layers grown by molecular beam epitaxy on GaAs(001) have been studied. We found that the Co_2FeSi layers have a long-range atomic order and crystallize in a partly disordered $L2_1$ structure in the low growth temperature (T_G) regime. The long-range atomic order of the layers is further improved with increasing T_G up to 350 °C. However, the increase of T_G induces an interfacial reaction between the Co_2FeSi layer and the GaAs substrate. The analysis of the in-plane magnetic anisotropy reveals that the interface perfection is improved up to T_G=200 °C and deteriorated due to an interfacial reaction above 200 °C. © *2005 American Institute of Physics*. [DOI: 10.1063/1.2136213]

I. INTRODUCTION

Spintronics (or spin electronics) is a recently emerging field of device concepts which is based on the spin degree of freedom of the electron, and is expected to lead to dramatic improvements in device performance. One of the key issues for the realization of spintronic devices is the efficient electrical injection of spin-polarized carriers into semiconductors. Electrical spin injection has been investigated mainly with Mn-doped III-V and II-VI semiconductors[1,2] and with conventional ferromagnetic metals.[3–6] Recently, Heusler alloys are of increasing interest as a candidate for a spin injection source into semiconductors, because of their high Curie temperature (from 200 to 1100 K), their compatibility with compound and element semiconductors, and half-metallicity predicted for some Heusler alloys.[7–10] There are a few reports of epitaxial Heusler alloys grown on semiconductor substrates, e.g., the full-Heusler alloys Co_2MnX (X=Ge, Ga),[11,12] and Ni_2MnY (Y=In, Ga),[13,14] as well as the half-Heusler alloy NiMnSb.[15,16] In addition, the growth of the binary Heusler alloy Fe_3Si on GaAs was reported[17,18] and a high crystal and interface perfection in the Fe_3Si layers was demonstrated in the proper growth temperature range.[17] More recently, electrical spin injection from Fe_3Si (Ref. 19) and Co_2MnGe (Ref. 20) was demonstrated. However, no evidence of a high degree of spin polarization as expected from theory has been observed in Heusler alloy films, up to now around 60% at maximum.[21–23]

In ferromagnet/semiconductor (FM/SC) heterostructures, mainly two obstacles with respect to their crystal structure are considered to prevent efficient electrical spin injection. One is the existence of interfacial compounds formed by diffusion of As and/or Ga into the FM layers, resulting in spin-flip scattering at the interface. The second is atomic disorder, such as vacancies and antisites. This disorder introduces minority gap states, and it was reported that only a few percent of antisite disorder can destroy the half-metallic nature of Heusler alloys.[24] Therefore, a highly atomically ordered, stoichiometric, and thermally stable thin film is needed for spin injection sources.

Co_2FeSi is a member of full-Heusler alloys with the cubic $L2_1$ crystal structure consisting of four interpenetrating fcc sublattices.[25] The lattice constant of bulk Co_2FeSi is 5.658 Å,[26] closely lattice matched to GaAs (a_{GaAs}=5.653 Å), and the lattice mismatch is as small as 0.08%. $Fe_{3-x}Co_xSi$ crystallizes in the cubic fcc structure in a wide range of x ($0<x<2.15$).[26] This phase stability allows control of the magnetic properties; e.g., magnetic anisotropy and magnetic moment. Bulk Co_2FeSi with a large magnetic moment (5.91 μ_B at 10.2 K) is ferromagnetic up to more than 980 K,[26] which is one of the highest Curie temperatures among the reported Heusler alloys. Here, we present a detailed study of the thermal stability and atomic ordering of single-crystal Heusler alloy Co_2FeSi films grown on GaAs (001) substrates by molecular beam epitaxy (MBE). The structural, electrical, and magnetic properties of Co_2FeSi films with various Si compositions and grown at different temperatures were systematically investigated.

II. SAMPLE PREPARATION

Before the growth of the Co_2FeSi layers, 100 nm thick GaAs templates were prepared in the III-V growth chamber using standard GaAs growth conditions. As-terminated $c(4\times4)$ reconstructed GaAs (001) surfaces were prepared by cooling the samples down to 420 °C under As_4 pressure to prevent the formation of macroscopic defects on the surface.[27] The samples were then transferred to the As-free deposition chamber under UHV at a base pressure of 5×10^{-10} Torr. The growth temperature T_G for the Co_2FeSi layers was varied in the range 100-400 °C to find the optimum growth temperature regime. A low growth rate of about 0.1 nm/min was chosen in order to avoid the degradation of the crystal quality at these low growth temperatures. The thickness of the layers d was determined by high-resolution x-ray diffraction (HRXRD) and x-ray reflectivity (XRR) measurements, and it varies in the range from 17 to 23 nm in accordance with the increase of T_{Si}. The growth was *in situ* monitored using reflection high-energy electron diffraction (RHEED). The RHEED pattern of the Co_2FeSi layer shows a rather spotty pattern at low T_G. The pattern gradually changes to sharp streaks with Kikuchi lines and a Laue circle

0021-8979/2005/98(10)/104902/6/$22.50

© 2005 American Institute of Physics

Downloaded 16 Dec 2005 to 62.141.165.15. Redistribution subject to AIP license or copyright, see http://jap.aip.org/jap/copyright.jsp

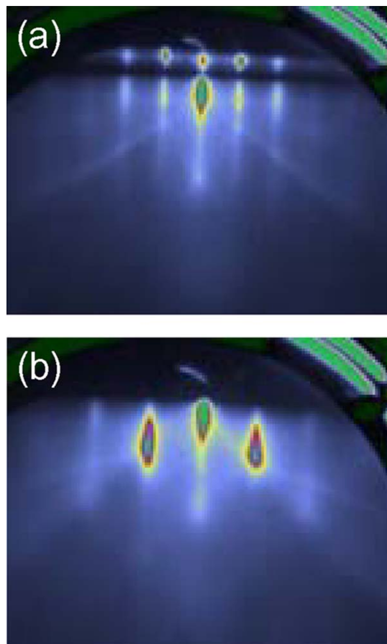

FIG. 1. (Color online) RHEED patterns of the Co_2FeSi layer grown at 250 °C along the (a) [110] and (b) [100] crystallographic directions during growth.

with increasing T_G, indicating a two-dimensional growth mode and a well-ordered single-crystal surface. Figure 1 shows typical RHEED patterns of Co_2FeSi film grown at 250 °C along the [110] and [100] crystallographic directions. After deposition of about 1–2 ML of the Co_2FeSi layer, an elongated streak pattern emerges. The pattern subsequently changes to sharp streaks and the streaky pattern is established during the deposition of about 3–6 ML of the Co_2FeSi layer. Then, the situation is maintained throughout the further growth.

The stoichiometric composition of Co_2FeSi was determined in the following way. First, the growth conditions of the binary alloy $Co_{0.66}Fe_{0.34}$ (bcc structure) were optimized. The composition of $Fe_{0.66}Co_{0.34}$ layers was determined by comparing the lattice constant with literature data,[28] taking into account the tetragonal distortion of the layers. Then, Si was added and incorporated to obtain ternary $Co_{2-x}Fe_ySi_{1+x+y}$ films, while the Fe and Co fluxes were kept constant at the optimized amounts. The Si cell temperature T_{Si} was varied from 1280 to 1335 °C to find the stoichiometric composition of Co_2FeSi. The perpendicular lattice mismatch $(\Delta a/a)_\perp$ of these $Co_{2-x}Fe_ySi_{1+x+y}$ films were subsequently examined by HRXRD using the $Co_2FeSi(004)$ reflection. From the value of $(\Delta a/a)_\perp$, the lattice constants of $Co_{2-x}Fe_ySi_{1+x+y}$ films were obtained, taking into account the tetragonal distortion of the layer, as confirmed in a reciprocal space map around $Co_2FeSi(113)$ reflections. Finally, from a comparison with the lattice constant of bulk Co_2FeSi from the literature,[26] the stoichiometric composition of Co_2FeSi was determined. More details of the determination are described elsewhere.[29]

III. RESULTS AND DISCUSSION

A. Structural properties

The structural properties of the films were examined *ex situ* by HRXRD with a PANalytical X'pert diffractometer

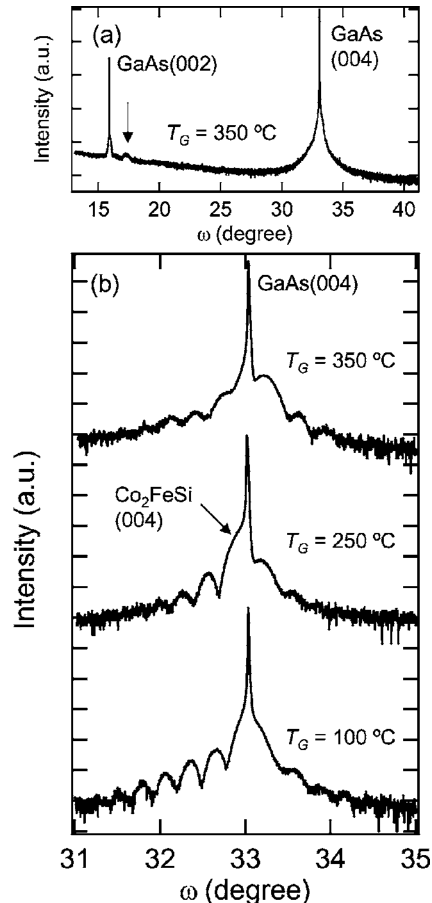

FIG. 2. HRXRD ω-θ curves around the $Co_2FeSi(004)$ reflection for stoichiometric $Co_2FeSi/GaAs(001)$ films grown at substrate temperature ranging from 100 to 350 °C. For the growth temperature of 350 °C, a wide-ranged ω-2θ curve with a wide-open detector is shown in the upper panel.

using Cu K_α radiation with a Ge(220) monochrometer and a triple-bounce analyzer crystal. Figure 2 shows the results of HRXRD ω-2θ curves of the $Co_2FeSi(004)$ reflection of stoichiometric Co_2FeSi films grown at different growth temperatures between 100 °C and 350 °C. In the lower growth temperature regime, high orders of interference fringes (up to fifth order) are seen, indicating a high crystal quality and interface perfection as well as a smooth surface. At T_G=250 °C, the interference fringes become less pronounced, indicating the onset of crystal degradation. At T_G=350 °C, the main peak is broadened and shifted to a larger angle, most likely due to an interfacial reaction. This was further evidenced by wide-range ω-2θ scans with a wide-open detector for the same series of films. An additional peak appears at around ω=17.3° for films grown above 350 °C, as is seen in the upper panel of Fig. 2 (arrows). We ascribe this peak to the $(Co,Fe)_2As(110)$ reflection caused by interfacial reaction between the Co_2FeSi layer and the GaAs substrate. Note that, based on these HRXRD results, the growth temperature at which an interfacial compound is formed is much higher than that of Fe, Co, and FeCo on GaAs.[27] This fact makes Co_2FeSi much more suitable for device applications than those ferromagnetic metals. However, since it is very difficult to detect nanometer-size interfacial compounds or clusters by XRD, further investiga-

Downloaded 16 Dec 2005 to 62.141.165.15. Redistribution subject to AIP license or copyright, see http://jap.aip.org/jap/copyright.jsp

tions of the interface perfection by an analysis of the in-plane magnetic anisotropy will be described later.

To confirm the atomic ordering of the films, additional reflections, namely the (002) and (113) reflections, were recorded. For the $L2_1$ structure, three types of reflections are allowed: (i) h, k, l are all odd [e.g., (113) reflection]; (ii) h, k, l are all even and $h+k+l=4n+2$ [e.g., (002) reflection]; and (iii) h, k, l are all even and $h+k+l=4n$ [e.g., (004) reflection], where n is an integer and h, k, l are the Miller indices of the diffracting plane. Type (iii) are the fundamental reflections which are not influenced by disorder, and the other two are the order-dependent superlattice reflections.[25] Type (i) reflections are reduced to zero in the limit of a complete disorder between Si and Fe sublattices, which leads to the reduction of the crystal symmetry to the $B2$ (CsCl) structure. Type (ii) reflections, on the other hand, are reduced to zero in the limit of complete disorder between all three sublattices, resulting in a further reduction of the crystal symmetry to the $A2$ (bcc) structure. Figure 3 depicts (a) the ω-2θ curve around the $Co_2FeSi(002)$ reflection, and (b) the reciprocal space map around the $Co_2FeSi(113)$ reflection of a stoichiometric Co_2FeSi film ($d=18.5$ nm) grown at 100 °C, and (c) the line profile along the dotted line shown in Fig. 3(b). Two main results can be derived from the figures. First, the two superlattice reflections of the $L2_1$ structure, namely the (002) and (113) reflections, are clearly seen with interference fringes, indicating the presence of a long-range atomic ordering and the Heusler-type $L2_1$ structure even for low T_G. The superlattice reflections were observed for Co_2FeSi films grown at different T_{Si} (namely different Si composition) and T_G as well. For the determination of the precise ordering parameters, further analyses of the superlattice reflections are underway. However, since the (113) reflections were taken in a reciprocal space mapping, it is difficult to quantitatively analyze the development of atomic ordering depending on T_{Si} and T_G from the intensity of superlattice reflections with respect to that of the fundamental one. Therefore, we performed electrical resistivity measurements instead on the films grown at different T_{Si} and T_G, as described in the following paragraphs. Second, the perfectly oriented vertical fringes indicate that the epitaxially grown Co_2FeSi layers are fully strained. This situation is preserved at least up to $d=38$ nm as far as we have studied.

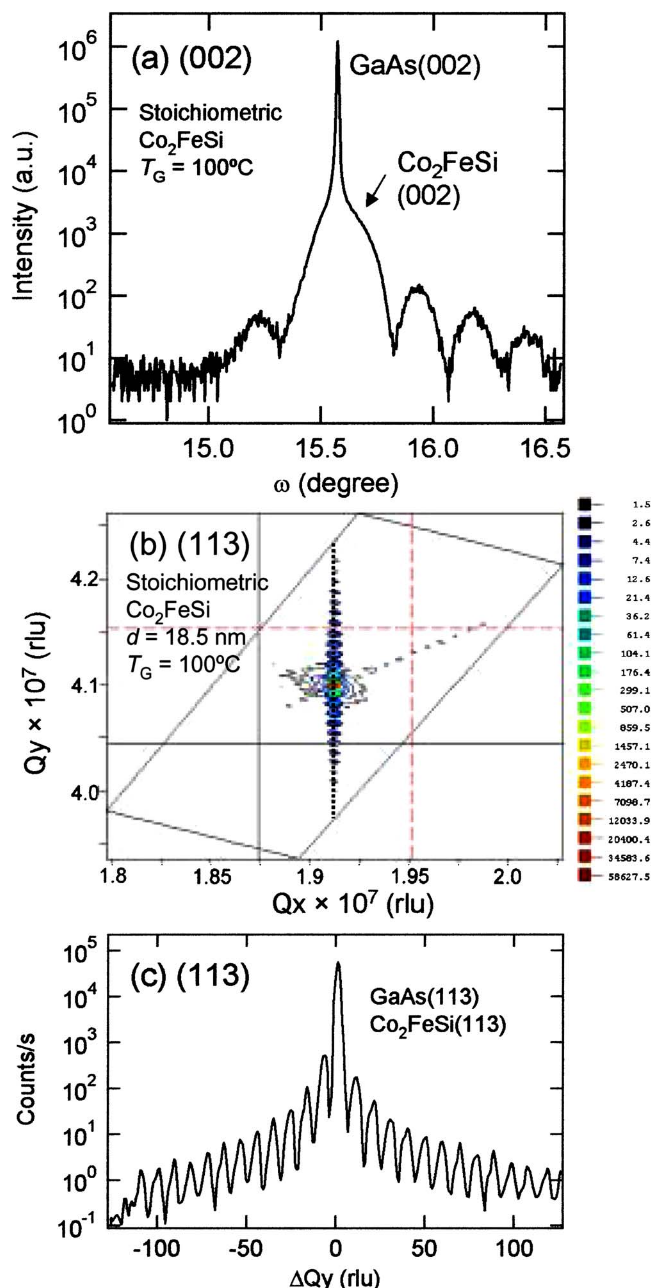

FIG. 3. (Color online) (a) HRXRD ω-2θ curve around $Co_2FeSi(002)$ reflection; (b) reciprocal space map around $Co_2FeSi(113)$ reflection; and (c) the line profile along the dotted line shown in (b) of a stoichiometric Co_2FeSi film grown at 100 °C.

B. Electrical properties

In order to obtain further information about atomic ordering of the Co_2FeSi films, we performed resistivity measurements on films with different Si compositions and T_G. Since the residual resistivity generally depends on the concentration of defects and impurities in the film, it can be used as a benchmark for evaluating the quality of alloy films. The resistivity of the Co_2FeSi films was measured using van der Pauw and Hall bar structures at two temperatures (77 and 300 K). The results are displayed in Fig. 4(a) together with that for $Co_{0.66}Fe_{0.34}$ (Si=0%). The broken line indicates the stoichiometric composition of Co_2FeSi determined by the lattice constant. The resistivity of the films monotonically increases with the Si composition. This is in contrast to the behavior expected for a perfectly ordered system, where the resistivity has a minimum at the stoichiometric composition due to the reduction of alloy scattering. This suggests that part of the Si atoms occupy inappropriate sublattice sites, namely the Co(A,C) and/or Fe(B) sites, resulting in Si antisite defects, although the majority of Si atoms occupies the Si(D) sites. Therefore, we conclude that the long-range atomic order and the $L2_1$ structure evidenced from the HRXRD results are not perfect due to the low growth temperature.

The long-range atomic order, however, is enhanced by elevating the growth temperature, as can be seen in Fig. 4(b). The figure shows the growth temperature dependence of the

Downloaded 16 Dec 2005 to 62.141.165.15. Redistribution subject to AIP license or copyright, see http://jap.aip.org/jap/copyright.jsp

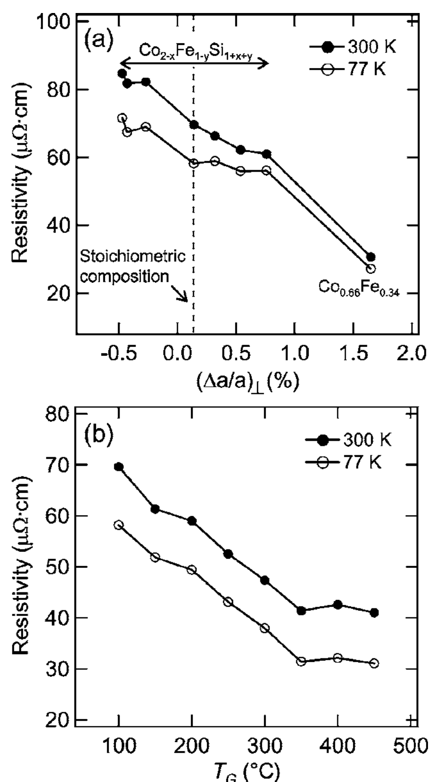

FIG. 4. Resistivity of Co_2FeSi films with (a) different Si compositions together with that of $Co_{0.66}Fe_{0.34}$ film and (b) different growth temperature measured on van der Pauw and Hall bar structures at 77 and 300 K. The broken line indicates the stoichiometric composition of Co_2FeSi determined by the lattice constant.

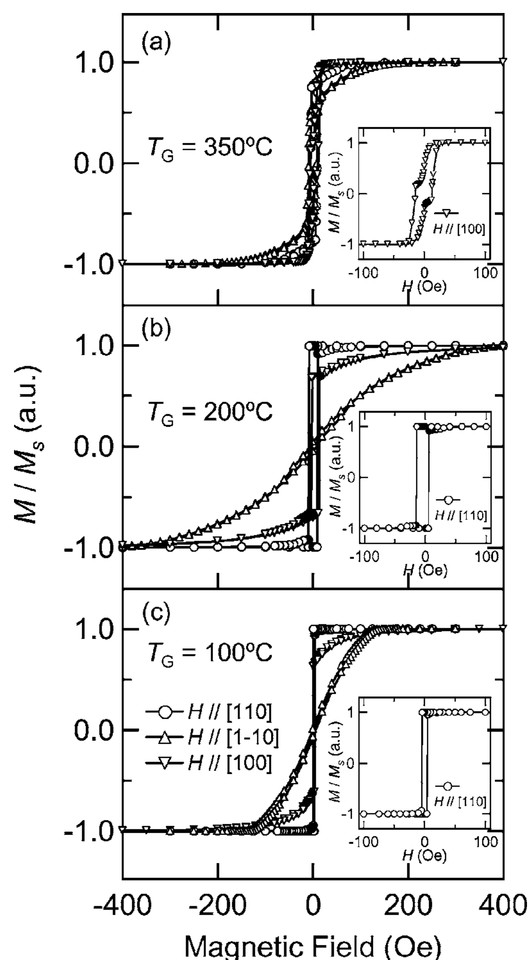

FIG. 5. Normalized magnetization curves of 18.5 nm thick stoichiometric Co_2FeSi/GaAs(001) films grown at (a) 350 °C; (b) 200 °C; and (c) 100 °C. All the measurements were performed at room temperature. The external magnetic field was applied along three crystallographic axes ([110], [$1\bar{1}0$], and [100] directions). The insets show expanded views of the magnetization curves along the easy axis. After subtraction of the diamagnetic contribution from the GaAs substrate, the magnetizations were normalized to the saturation magnetization of each direction.

resistivity for stoichiometric Co_2FeSi films. The decrease of the resistivity with increasing T_G up to 350 °C demonstrates the improvement of the atomic ordering of crystal structure. The crystalline quality of the bulk structure, therefore, is better at higher T_G, in clear contrast to that of the interface structure where higher T_G results in interfacial reactions, as we have seen in the HRXRD results. Therefore, the optimum growth temperature for Co_2FeSi/GaAs lies in the regime where the crystalline quality of the interface and the bulk structure are compromised.

C. Magnetic properties

The in-plane magnetic anisotropy of Co_2FeSi/GaAs heterostructures was investigated using superconducting quantum interference device (SQUID) magnetometry. All measurements were performed at room temperature. The external magnetic field was applied along three crystallographic axes, namely the [110], [$1\bar{1}0$], and [100] directions. After subtraction of the diamagnetic contribution of the GaAs substrate, the magnetizations were normalized to the saturation magnetization of each direction. All examined Co_2FeSi films are ferromagnetic at room temperature. In Fig. 5, we show the normalized magnetization curves of the stoichiometric Co_2FeSi films grown at (a) 350 °C, (b) 200 °C, and (c) 100 °C and the expanded views along the easy axis in the inset. Two main results can be derived from the measurements.

First, the shape of the magnetization curves and the angle dependence of the magnetization dramatically change at T_G=350 °C. The magnetization curves of T_G<200 °C show square-shaped hysteresis loops and strongly anisotropic angle dependences. The magnetization curves of T_G<200 °C exhibit an easy axis [110], a hard axis [$1\bar{1}0$], and an intermediate axis [100]. The easy axis along the [110] direction is caused by a dominating uniaxial in-plane magnetic anisotropy component which has an easy axis different from that of the cubic magnetocrystalline anisotropy component (⟨100⟩ directions). The well-defined square-shaped hysteresis loop along the [110] direction with a small coercive field of 4.5 Oe confirms the excellent crystal quality of the films. The saturation magnetization M_s of stoichiometric films amounts to 1250±120 emu/cm^3, which is relatively close to that of bulk Co_2FeSi [1124 emu/cm^3 at 295 K (Ref. 26)], confirming the stoichiometric composition determined from the lattice constant. The M_s value decreases with increasing T_G, most likely due to the formation of a magnetically modified layer at the interface. The magnetiza-

Downloaded 16 Dec 2005 to 62.141.165.15. Redistribution subject to AIP license or copyright, see http://jap.aip.org/jap/copyright.jsp

tion curve of the T_G=350 °C sample, on the other hand, changes to a nearly isotropic angle dependence. The uniaxial anisotropy component almost disappears and the cubic term remains. The easy axis in total is consequently converted to the easy axis of the cubic component: the $\langle 100 \rangle$ direction. Note that the double steplike loop of the easy axis of the T_G=350 °C sample seen in the inset of Fig. 5(a) originates from a slight deviation of the easy axis from the $\langle 100 \rangle$ directions due to the remaining slight uniaxial component.

Second, the in-plane magnetic anisotropy significantly increases with elevating T_G from 100 to 200 °C. The in-plane magnetic anisotropy of Co_2FeSi films was analyzed, assuming that a free-energy density consists of a cubic magnetocrystalline anisotropy term K_1^{eff} and a uniaxial anisotropy term K_u^{eff} (Ref. 30)

$$\varepsilon(\phi) = -\frac{1}{4}K_1^{\text{eff}} \sin^2(2\phi) + K_u^{\text{eff}} \sin^2(\phi) - HM_s \cos(\phi - \alpha), \quad (1)$$

where α is the angle between external field H and the [110] direction, and ϕ is the angle between magnetization and the [110] direction. Assuming a coherent rotation as a magnetization reversal process, the relation between magnetic field and magnetization is given by minimizing $\varepsilon(\phi)$ (Ref. 30)

$$H(m) = 2K_1^{\text{eff}}(2m^3 - m)/M_s + 2K_u^{\text{eff}} m/M_s, \quad (2)$$

where $m = \sin(\phi)$ is the normalized magnetization component. By fitting the magnetization curves along the $[1\bar{1}0]$ direction with this expression, two effective magnetic anisotropy constants, K_1^{eff} and K_u^{eff}, were obtained. K_u^{eff} is plotted as a function of T_G in Fig. 6(a). As can be seen from the figure, K_u^{eff} reaches a maximum at around T_G=200 °C and decreases with the further increase of T_G. The value of K_u^{eff} finally becomes almost negligible at T_G=350 °C. Note that the value of K_u^{eff} at T_G=350 °C is not plotted in Fig. 6(a), since it cannot be obtained analytically due to the absence of a reversible hard axis.

In general, K_u^{eff} and K_1^{eff} can be decomposed assuming a superposition of a volume term $K_{u,1}^{\text{vol}}$ and an interface contribution $K_{u,1}^{\text{int}}$,

$$K_{u,1}^{\text{eff}} = K_{u,1}^{\text{vol}} + K_{u,1}^{\text{int}}/d, \quad (3)$$

where d is the thickness of the film.[30] We plot K_u^{eff} and K_1^{eff} vs inverse d of Co_2FeSi films grown at 100 °C in Fig. 6(b). K_1^{eff} is independent of d, indicating that K_1^{eff} is a volume-related term, whereas K_u^{eff} is linearly dependent on inverse d. As obtained from the fit, K_u^{vol} is nearly zero and $K_u^{\text{int}} = (7.3 \pm 0.9) \times 10^{-2}$ erg/cm^2, demonstrating that K_u^{eff} is a pure interface-related term, as is observed in other FM/SC systems. The value of K_u^{int} is in between those of Fe (Ref. 31) and $Fe_{0.34}Co_{0.66}$ (Ref. 30) on GaAs: 1.2×10^{-1} and 2.6×10^{-2} erg/cm^2, respectively. Since the value of K_u^{int} has been estimated from a series of films grown at 100 °C, namely at the lowest end of the low T_G regime in Fig. 5(a), K_u^{int} can be expected to be larger at higher T_G. In general, the uniaxial in-plane magnetic anisotropy observed in FM/SC systems is anticipated to originate from an anisotropic bonding at the interface.[32] Therefore, the T_G dependence of K_u^{eff} reflects the interface perfection including atomic ordering and abruptness. Hence, the quality of the interface is improved with the increase of T_G up to 200 °C, and then it deteriorates due to the interfacial reaction for $T_G > 200$ °C. Thus, we conclude from the analysis of the in-plane magnetic anisotropy that the optimum T_G to obtain a perfect interface structure is around 200 °C.

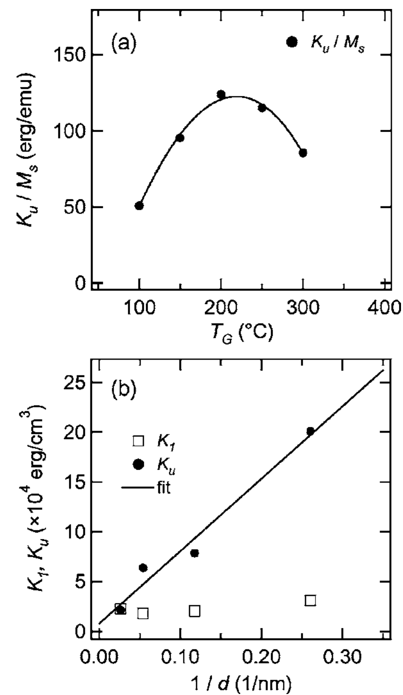

FIG. 6. (a) Uniaxial magnetocrystalline anisotropy constant (K_u^{eff}/M_s) of stoichiometric Co_2FeSi films as a function of growth temperature. (b) Uniaxial and cubic magnetocrystalline anisotropy constants (K_u^{eff} and K_1^{eff}, respectively) as a function of inverse film thickness d. The solid line shows the linear fit for K_u^{eff}.

IV. CONCLUSIONS

In conclusion, we have grown single-crystal full-Heusler alloy Co_2FeSi films on GaAs (001) by molecular beam epitaxy. Co_2FeSi layers with high crystal and interface perfection as well as smooth surfaces can be obtained by carefully controlling the fluxes of Co, Fe, and Si. The HRXRD and resistivity studies revealed that the layers have a long-range order and crystallize in a partly disordered Heusler-type $L2_1$ structure in the low growth temperature regime. The long-range atomic order of the layers is improved by elevating the growth temperature up to 350 °C. The increase of the growth temperature, however, results in an interfacial reaction between the Co_2FeSi layer and the GaAs substrate. The analysis of the in-plane magnetic anisotropy revealed that the interface perfection improves up to T_G=200 °C and deteriorates due to interfacial reactions above 200 °C. The optimum growth temperature for Co_2FeSi/GaAs heterostructures with high interface and crystal perfection, as well as high degree of atomic ordering, is thus around 200 °C. Hence, Co_2FeSi films are much more thermally stable than conventional ferromagnetic metals on GaAs. These results

Downloaded 16 Dec 2005 to 62.141.165.15. Redistribution subject to AIP license or copyright, see http://jap.aip.org/jap/copyright.jsp

indicate that Heusler alloys are promising candidates as a source for efficient electrical spin injection into semiconductors.

ACKNOWLEDGMENTS

This work was partly supported by the German BMBF under the research program NanoQUIT (Contract No. 01BM463). The authors would like to thank P. K. Muduli for useful discussions, A. Riedel for technical assistance, and R. Koch for a careful reading of the manuscript.

[1]R. Fiederling, M. Keim, G. Reuscher, W. Ossau, G. Schmidt, A. Waag, and L. W. Molenkamp, Nature (London) **402**, 787 (1999).
[2]Y. Ohno, D. K. Young, B. Beschoten, F. Matsukura, H. Ohno, and D. D. Awschalom, Nature (London) **402**, 790 (1999).
[3]H. J. Zhu, M. Ramsteiner, H. Kostial, M. Wassermeier, H.-P. Schönherr, and K. H. Ploog, Phys. Rev. Lett. **87**, 016601 (2001).
[4]B. T. Jonker, A. T. Hanbicki, Y. D. Park, G. Itskos, M. Furis, G. Kioseoglou, A. Petrou, and X. Wei, Appl. Phys. Lett. **79**, 3098 (2001).
[5]X. Jiang, R. Wang, S. van Dijken, R. Shelby, R. Macfarlane, G. S. Solomon, J. Harris, and S. S. P. Parkin, Phys. Rev. Lett. **90**, 256603 (2003).
[6]T. Manago and H. Akinaga, Appl. Phys. Lett. **81**, 694 (2002).
[7]C. Palmstrøm, MRS Bull. **28**, 725 (2003).
[8]R. A. de Groot, F. M. Mueller, P. G. van Engen, and K. H. J. Buschow, Phys. Rev. Lett. **50**, 2024 (1983).
[9]I. Galanakis, P. H. Dederichs, and N. Papanikolaou, Phys. Rev. B **66**, 174429 (2002).
[10]S. Fujii, S. Sugimura, J. Ishida, and S. Asano, J. Phys.: Condens. Matter **2**, 8583 (1990).
[11]T. Ambrose, J. J. Krebs, and G. A. Prinz, Appl. Phys. Lett. **76**, 3280 (2000).
[12]S. N. Holmes and M. Pepper, Appl. Phys. Lett. **81**, 1651 (2002).
[13]J. Q. Xie, J. W. Dong, J. Lu, C. J. Palmstrøm, and S. Mckernan, Appl. Phys. Lett. **79**, 1003 (2001).
[14]M. S. Lund, J. W. Dong, J. Lu, X. Y. Dong, C. J. Palmstrøm, and C. Leighton, Appl. Phys. Lett. **80**, 4798 (2002).
[15]W. Van Roy, J. De Boeck, B. Brijs, and G. Borghs, Appl. Phys. Lett. **77**, 4190 (2000).
[16]P. Bach, A. S. Bader, C. Rüster, C. Gould, C. R. Becker, G. Schmidt, L. W. Molenkamp, W. Weigand, C. Kumpf, E. Umbach, R. Urban, G. Woltersdorf, and B. Heinrich, Appl. Phys. Lett. **83**, 521 (2003).
[17]J. Herfort, H.-P. Schönherr, and K. H. Ploog, Appl. Phys. Lett. **83**, 3912 (2003); J. Herfort, H.-P. Schönherr, K.-J. Friedland, and K. H. Ploog, J. Vac. Sci. Technol. B **22**, 2073 (2004).
[18]A. Ionescu, C. A. F. Vaz, T. Trypiniotis, C. M. Gürtler, H. García-Miquel, J. A. C. Bland, M. E. Vickers, R. M. Dalgliesh, S. Langridge, Y. Bugoslavsky, Y. Miyoshi, L. F. Cohen, and K. R. A. Ziebeck, Phys. Rev. B **71**, 094401 (2005).
[19]A. Kawaharazuka, M. Ramsteiner, J. Herfort, H.-P. Schönherr, H. Kostial, and K. H. Ploog, Appl. Phys. Lett. **85**, 3492 (2004).
[20]X. Y. Dong, C. Adelmann, J. Q. Xie, C. J. Palmstrøm, X. Lou, J. Strand, P. A. Crowell, J.-P. Barnes, and A. K. Petford-Long, Appl. Phys. Lett. **86**, 102107 (2005).
[21]S. Kämmerer, A. Thomas, A. Hütten, and G. Reiss, J. Appl. Phys. **85**, 79 (2004).
[22]L. J. Singh, Z. H. Barber, Y. Miyoshi, W. R. Branford, and L. F. Cohen, J. Appl. Phys. **95**, 7231 (2004).
[23]R. J. Soulen Jr., J. M. Byers, M. S. Osofsky, B. Nadgorny, T. Ambrose, S. F. Cheng, P. R. Broussard, C. T. Tanaka, J. Nowak, J. S. Moodera, A. Barry, and J. M. D. Coey, Science **282**, 85 (1998).
[24]S. Picozzi, A. Continenza, and A. J. Freeman, Phys. Rev. B **69**, 094423 (2004).
[25]For the details of $L2_1$ structure, see P. J. Webster and K. R. A. Ziebeck, *Landolt-Börnstein New Series III/19c* (Springer, Berlin, 1988), p. 75.
[26]V. Niculescu, T. J. Burch, K. Raj, and J. I. Budnick, J. Magn. Magn. Mater. **5**, 60 (1977); V. Niculescu, J. I. Budnick, W. A. Hines, K. Raj, S. Pickart, and S. Skalski, Phys. Rev. B **19**, 452 (1979).
[27]H.-P. Schönherr, R. Nötzel, W. Ma, and K. H. Ploog, J. Appl. Phys. **89**, 169 (2001).
[28]T. Nishizawa and K. Ishida, Bull. Alloy Phase Diagrams **5**, 250 (1984).
[29]M. Hashimoto, J. Herfort, H.-P. Schönherr, and K. H. Ploog, Appl. Phys. Lett. **87**, 102506 (2005).
[30]M. Dumm, M. Zölfl, R. Moosbühler, M. Brockmann, T. Schmidt, and G. Bayreuther, J. Appl. Phys. **87**, 5457 (2000).
[31]M. Brockmann, M. Zölfl, S. Miethaner, and G. Bayreuther, J. Magn. Magn. Mater. **198–199**, 184 (1999).
[32]E. Sjöstedt, L. Nordström, F. Gustavsson, and O. Eriksson, Phys. Rev. Lett. **89**, 267203 (2002).

Downloaded 16 Dec 2005 to 62.141.165.15. Redistribution subject to AIP license or copyright, see http://jap.aip.org/jap/copyright.jsp